

A Mystery in Chamaeleon: Serendipitous Discovery of a Galactic Symbiotic Nova

LACHLAN LANCASTER,¹ JENNY E. GREENE,¹ YUAN-SEN TING,^{2,1,3,4,*} SERGEY E. KOPOSOV,^{5,6,7} BENJAMIN J. S. POPE,^{8,9,†}
AND RACHAEL L. BEATON^{1,3,*}

¹*Department of Astrophysical Sciences, Princeton University, 4 Ivy Lane, 08544, Princeton, NJ, USA*

²*Institute for Advanced Study, Princeton, NJ 08540, USA*

³*Observatories of the Carnegie Institution of Washington, 813 Santa Barbara Street, Pasadena, CA 91101, USA*

⁴*Research School of Astronomy and Astrophysics, Mount Stromlo Observatory, Cotter Road, Weston Creek, ACT 2611, Australia*

⁵*McWilliams Center for Cosmology, Carnegie Mellon University, 5000 Forbes Avenue, 15213, Pittsburgh, PA, USA*

⁶*Institute of Astronomy, University of Cambridge, Madingley Road, Cambridge, CB3 0HA, UK*

⁷*Kavli Institute for Cosmology, University of Cambridge, Madingley Road, Cambridge CB3 0HA, UK*

⁸*Center for Cosmology and Particle Physics, Department of Physics, New York University, 726 Broadway, New York, NY 10003, USA*

⁹*Center for Data Science, New York University, 60 Fifth Ave, New York, NY 10011, USA*

(Received XXX; Revised XXX; Accepted February 20, 2020)

Submitted to AJ

ABSTRACT

We present the serendipitous discovery of a low luminosity nova occurring in a symbiotic binary star system in the Milky Way. We lay out the extensive archival data alongside new follow-up observations related to the stellar object V* CN Cha in the constellation of Chamaeleon. The object had long period (~ 250 day), high amplitude (~ 3 mag) optical variability in its recent past, preceding an increase in optical brightness by ~ 8 magnitudes and a persistence at this luminosity for about 3 years, followed by a period of ~ 1.4 mag yr⁻¹ dimming. The object's current optical luminosity seems to be dominated by H α emission, which also exhibits blue-shifted absorption (a P-Cygni-like profile). After consideration of a number of theories to explain these myriad observations, we determine that V* CN Cha is most likely a symbiotic (an evolved star-white dwarf binary) system which has undergone a long-duration, low luminosity, nova. Interpreted in this way, the outburst in V* CN Cha is among the lowest luminosity novae ever observed.

Keywords: stars, symbiotic binary, novae

1. INTRODUCTION

“One of the advantages to being disorganized is that one is always having surprising discoveries.”
- A.A. Milne (Milne 1956)

The array of human-collected astronomical data is vast. Varied in both structure and content, there is no single archive that gathers all such data in to a single, easily accessible place. Comparison between historical and contemporary datasets can reveal many previously-

overlooked astrophysical phenomena. In this paper, we present a dramatic outburst from the star V* CN Cha, whose enigmatic nature was only revealed through the broad temporal and spectral coverage available across astronomical archives.

On a recent observing run, we chose bright and distant objects from the *Gaia* DR2 data (Gaia Collaboration et al. 2016, 2018) for spectroscopic follow-up. One such candidate was the star V* CN Cha in the constellation of Chamaeleon. As we will outline below, the observations that followed were quite intriguing. Yet the archival data which had already been gathered on this object were even more fascinating, including variations in brightness over a range of ten magnitudes that occurred on a variety of time scales. This variation is

Corresponding author: Lachlan Lancaster
lachlanl@princeton.edu

* Hubble Fellow
Carnegie-Princeton Fellow

† NASA Sagan Fellow

exemplified in Figure 1, which shows observations of V* CN Cha separated by 25 years.

In Section 2 we present and summarize the set of archival data pertaining to this object. We then present the optical spectrum that we observed for V* CN Cha in Section 3. After having presented the data we provide more detailed analysis of various parts of the data in Section 4. Using the net sum of the observational data we then discuss the possible theories that could explain them in Section 5. Among these theories, we determine that it is likely that V* CN Cha is a symbiotic nova. In Section 6 we briefly discuss the implications of the interpretation of V* CN Cha as a symbiotic nova on the study of novae. Finally, we discuss possible follow-up observations that could be taken of this object and conclude in Section 7.

2. ARCHIVAL DATA

We present the various archival data that we have gathered on this object. We begin with a summary of the data as a whole. This is followed by a detailed description of each constituent data set, beginning with the *Gaia* data on the object, which first motivated our investigation. We then present the numerous archival photometric observations, roughly in chronological order, so as to give the reader a full explanation of the data underlying the photometric variability.

2.1. Archival Summary

V* CN Cha was first identified as a Mira variable in 1963 and was observed by multiple surveys throughout the 20th century which took measurements consistent with this initial conclusion. A visual summary of the photometric data since 2000 is given in Figure 2. We gather multi-epoch photometry spanning nearly 20 years ranging from the near UV to the far infrared. The information summarized in Figure 2 indicates that V* CN Cha experienced an outburst event at some point in 2013. We find that the pre-outburst SED is best described by the sum of two blackbodies, one cool (2000 K) bright component, and one hot (10000 K) dim component. Observing the SEDs from before and after this event, it is clear that the object became much brighter in almost all bands for which we can make a reasonable comparison. This brightness difference is most extreme in the UV where an observed increase in flux by a factor of 10,000 is seen between UVOT and SkyMapper measurements. It should be noted that these SkyMapper measurements in the UV were taken very soon after the outburst event, in March of 2014, so it is plausible to assume that the SED now is somewhat different than it was then, especially given the dimming that was observed later in the ASAS-SN lightcurve.

Finally, we show the TESS lightcurve in Figure 3, which we classify as ‘archival’ despite the fact that it was taken after our own observation. The main conclusions from the TESS data are that (1) they indicate that the star is still steadily dimming at a rate consistent with the ASAS-SN observations and (2) they suggest the star has short-term variability on the timescale of several hours.

2.2. *Gaia*

The European Space Agency’s astrometric space mission *Gaia*, observed V* CN Cha during its first window of observation used in the mission’s second data release (DR2) (DR2 *Gaia* Collaboration et al. 2016, 2018). This observation window was from July 24th, 2014 to May 23rd, 2016. The mission observed the star to be peculiar in a number of ways that alerted the authors that the star may be interesting. The key observations that piqued our interest were:

1. The photometric observations gave $G = 7.41$, $G_{BP} = 7.72$, $G_{RP} = 6.98$ mag, making the star relatively bright.

2. The star was assigned a parallax of

$$\varpi = 0.3142 \pm 0.0249 \text{ mas} \quad (1)$$

putting the star’s distance at $3.18^{+0.27}_{-0.23}$ kpc, implying an absolute G band magnitude of -5.1 mag, making it unusually luminous.

3. The astrometric pipeline assigned zero astrometric excess noise (AEN) to this object, which indicates that the astrometry does not show obvious problems. The Renormalized Unit Weight Error (RUWE) is 1.19.
4. The star was not classified as variable.

The first three of the above items were enough to identify this object as one of interest for follow-up.

2.3. Identification

V* CN Cha was first identified as a Mira variable star in 1963 as reported by Hoffmeister (1963). At that time the star was identified to vary between magnitude 15 and 17¹, in the Johnson I band.

2.4. IRAS

The star was later identified by the Infrared Astronomical Satellite (IRAS) as a strong point source in

¹ www.sai.msu.su/gcvs/cgi-bin/search.cgi?search=CN+Cha

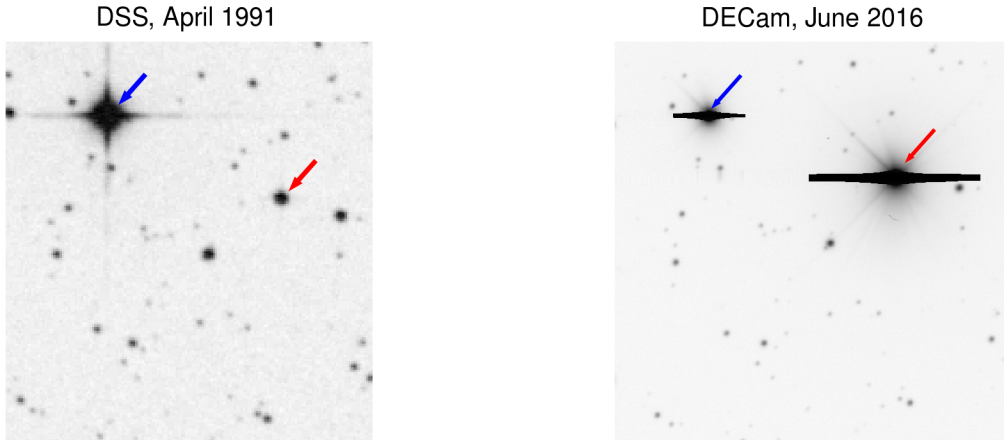


Figure 1. We show a comparison of two images of V^* CN Cha, which is indicated by a red arrow in both panels. The left panel shows the DSS R band observation taken in April of 1991 and the right shows the DECam r band observation taken in June of 2016. Despite the fact that the images are at different contrast levels and resolutions, and they are taken in slightly different bands, it is clear from comparison to the nearby star CD-79 452 (indicated with a blue arrow) that V^* CN Cha has increased in brightness considerably.

all four bands (12, 25, 60, and 100 μm) as well as being given an 82% probability of being variable based on analysis of the 12 and 25 micron flux densities and their uncertainties (Neugebauer et al. 1984).

2.5. Hipparcos

Despite being very bright in the optical at the current epoch, it was not recorded as a source in any of the catalogues created from observations performed by the Hipparcos satellite (Hip 1997; Høg et al. 2000). The completeness of the Tycho-2 catalog is 99% for stars brighter than 11 magnitude in the V band (Høg et al. 2000), suggesting that V^* CN Cha was likely dimmer than 11th magnitude in the V band during Hipparcos’s observations from 1989 to 1993.

2.6. Digitized Sky Survey

The Digitized Sky Survey (DSS) consists of a series of photometric plate observations done on the Oschin and UK Schmidt Telescopes between 1983 and 2006 (Lasker et al. 1996, 1990). V^* CN Cha was observed by the UK Schmidt Telescope using the RG610 filter (approximating the Johnson-Cousins R band) on April 12th, 1991. We show this observation in the left hand panel of Figure 1. The star was reported to have magnitude $\text{RG610}=13.26$ mag in this band by the DSS (Lasker et al. 1990).

The star was also observed by the DSS in January of 1976 in a GG395 filter at a bluer wavelength and in March of 1996 in a RG715 filter at a redder wavelength.

While these exposures are available online², we could not determine zero-point fluxes for stars in these bands or stars within the field with reference magnitudes in these bands, so we do not report any photometry for these images.

2.7. Deep Near Infrared Survey

The Deep Near Infrared Survey (DENIS) was a near infrared survey operated out of the 1-meter European Southern Observatory (ESO) telescope at La Silla, Chile (Epchtein et al. 1994). DENIS also gathered multiple observations of 355 million objects in each of its three bands: I (0.8 μm), J (1.2 μm), and K_s (2.1 μm) (Fouqué et al. 2000). The DENIS survey observed V^* CN Cha on three occasions from early 1999 to January of 2000 (DENIS Consortium 2005). However all observations in the J and K_s bands were brighter than the saturation limits of the DENIS survey, as was the second observation in the I band (Epchtein et al. 1994). For this reason we only use the two DENIS observations in the I band that were unsaturated. The range of flux that these observations cover is indicated in Figure 2.

2.8. Two-Micron All Sky Survey

The Two-Micron All Sky Survey (2MASS) was a full-sky survey in the J , H (1.65 μm), and K_s bands operated on two dedicated 1.3 meter telescopes at Mount Hopkins, Arizona and Cerro Tololo, Chile between June of 1997 and February of 2001. The survey was estimated

² https://archive.stsci.edu/cgi-bin/dss_form

to be complete at signal-to-noise greater than 10 to approximately 15th magnitude in the H band. V* CN Cha was observed by 2MASS on January 13th, 2000 (Skrutskie et al. 2006).

2.9. All Sky Automated Survey

The All Sky Automated Survey (ASAS) was designed as one of the first major efforts to obtain time-variability information on a large fraction of stars in the night sky (Pojmanski 1997). The ASAS survey obtained observations of V* CN Cha from November 21st, 2000 to November 27th, 2009 (Pojmanski 2002a, 2003, 2004). The light curve for the star is reported in two separate online catalogues that we were able to find. We use both catalogues, as they seem consistent with one another, and discuss the relation between them in Appendix A.

The ASAS survey used these observations to identify V* CN Cha as a Mira variable star with a period of 260 days. The light curves from the original ASAS survey were reanalyzed in 2016 by Vogt et al. (2016) with more rigorous analysis techniques. In this reanalysis, V* CN Cha has a period of 253.24 days.

2.10. Radial Velocity Experiment

The Radial Velocity Experiment (RAVE) obtained a spectrum of V* CN Cha on February 20th, 2010 (Kordopatis et al. 2013). The RAVE team very generously provided us with a copy of the spectrum taken in 2010 in advance of its planned release in 2020. The star's spectrum shows clearly very low T_{eff} with broad TiO absorption features, consistent with a cool giant star. Unfortunately, the RAVE pipeline fits seem to have hit the boundary of the stellar parameter grids and therefore extracted stellar model parameters are not reliable (RAVE Team, private communication). We leave the analysis of this spectrum to future work.

2.11. AKARI

The AKARI satellite was a Japanese astronomical all-sky survey in six infrared bands between $9\mu\text{m}$ and $200\mu\text{m}$ (Murakami et al. 2007). This survey was carried out between May 6th, 2006 and August 8th, 2007, during which time AKARI observed V* CN Cha and reported measurements for its flux in band passes centered at $9\mu\text{m}$ and $18\mu\text{m}$ and non-detections in all longer wavelength bands at 65, 90, 140, and $160\mu\text{m}$ (Yamamura et al. 2010).

2.12. Swift/UVOT

The Neil Gehrels *Swift* Observatory is a space observatory mission directed by NASA and built for the

main purpose of detecting Gamma Ray Bursts (GRBs)³. The *Swift* UV and Optical Telescope (UVOT) observes the sky in four broad bands $UVW2(1928\text{\AA})$, $UVM2(2246\text{\AA})$, $UVW1(2600\text{\AA})$, and $U(3465\text{\AA})$ spanning the far to near UV (Kuin et al. 2015). Data from UVOT was used to create the *Swift*/UVOT Serendipitous Source Catalog (SUVOTSSC) which catalogs a number of point sources in these bands (Yershov 2014; Page et al. 2014). V* CN Cha was observed six times by UVOT and we display the photometry from January of 2008 in Figure 2.

2.13. APASS

The American Association of Variable Star Observers (AAVSO) Photometric All-Sky Survey (APASS) is a survey performed primarily in five bands: Johnson-Cousins B and V as well as Sloan g' , r' , and i' (Henden et al. 2009; Henden & Munari 2014). With their latest data release (DR10), there have been observations in the Sloan u' and z' bands as well as the Y band (Henden et al. 2018).

The epoch photometry from the APASS survey is also available through the AAVSO's International Variable Star Index (VSX)⁴. The VSX data includes g' , r' , and i' values for 5 epochs spanning from March 26th, 2012 to April 5th 2014. The last three of these 5 epochs additionally have photometric measurements in the B , V , and z' bands. This photometric information was essential in constraining the behaviour of V* CN Cha in an otherwise unobserved portion of its evolution as shown in Figure 2, where we can see its rise in luminosity from magnitude 16 to magnitude 8.

As we have the most information on the long-term variability of V* CN Cha in the V -band, in order to have the largest number of epochs for comparison we use the APASS g' and r' bands to calculate an effective V band magnitude for the two earliest observations where there is no directly measured V band magnitude. The calibration we use is

$$V = g' - 0.52(g' - r') - 0.03 \text{ mag}, \quad (2)$$

which comes from Jester et al. (2005). It should be noted that this relation is derived using relatively well behaved stars, so our use of the relation here for such a strange object as V* CN Cha may not be ideal.

2.14. WISE

The Wide-field Infrared Survey Explorer (WISE) observed V* CN Cha on February 20th and 27th of 2010,

³ <https://swift.gsfc.nasa.gov>

⁴ <https://www.aavso.org/vsx/>

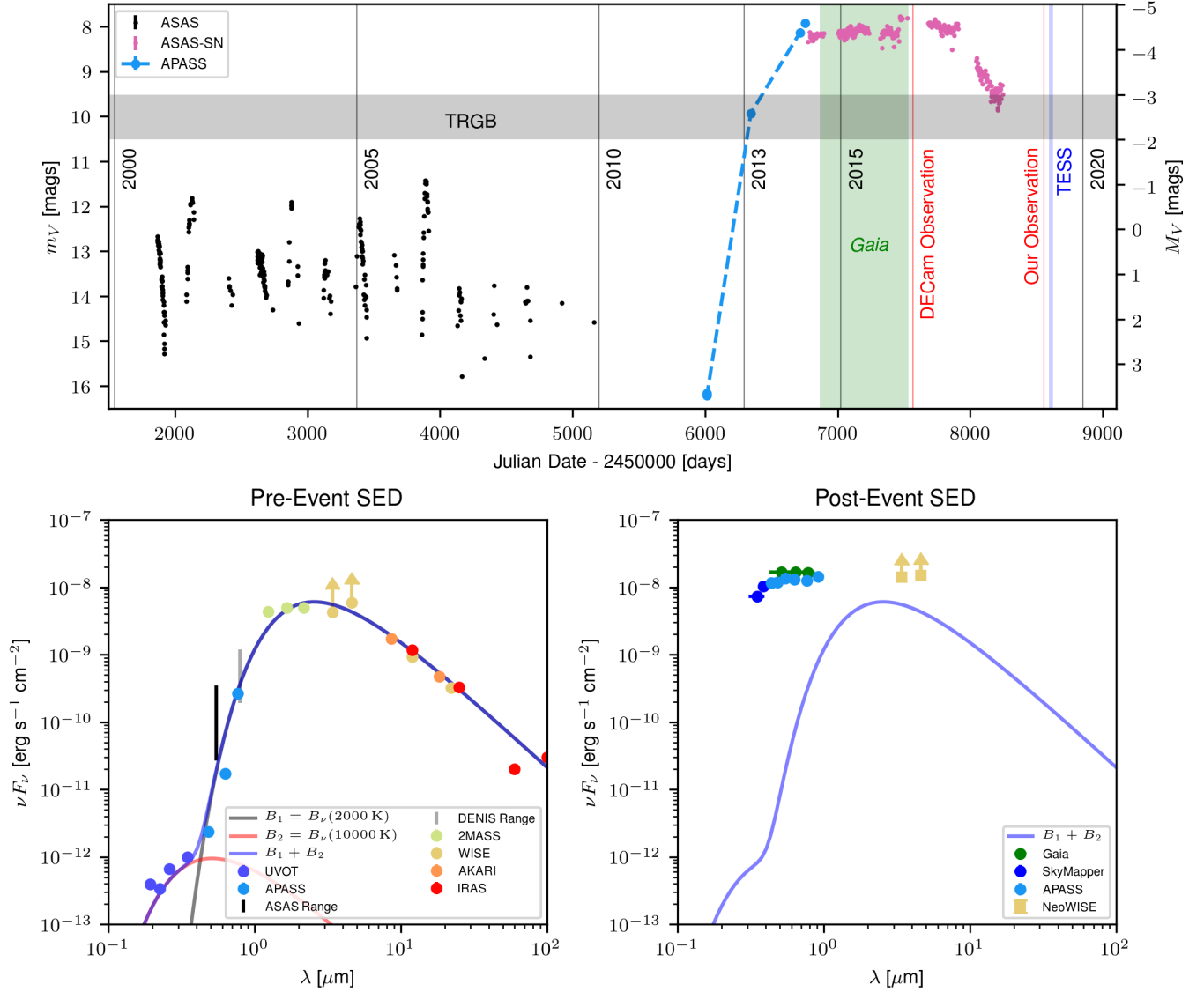


Figure 2. A summary of the photometric data. *Top Panel:* We show a combination of light curves from the ASAS survey (black points), the APASS survey (light-blue points connected by a dashed line) and the ASAS-SN survey (pink points) all in approximations of the Johnson-Cousins V -band; we make no correction for marginal differences in the definitions of these bands between surveys. The scale for the apparent (absolute, from *Gaia* parallax) magnitude is shown at left (right). We indicate intervals of 5 years (along with 2013, the year we believe the outburst occurred) with vertical grey lines, the DECcam and our spectroscopic observations as vertical red lines, and the period over which the *Gaia* mission used data for its DR2 as a green band. The small blue band indicates the TESS observations. We indicate the typical range in absolute magnitude spanned by the tip of the red giant branch (TRGB) as a horizontal grey band. *Bottom Left Panel:* We show an SED for the star for photometric data that is determined to have been taken ‘pre-event.’ We compare the data with an SED which is the sum of two blackbody spectra, one with a temperature of 10,000 K and one with a temperature of 2000K for reference, the normalization of this spectrum was chosen to marginally follow the observed photometric data. We chose two blackbodies to match the UV excess observed in the data. As the star is observed to vary quite strongly in the ‘pre-event’ phase we attempt to illustrate this variability by indicating the range of variability of the ASAS V band measurements as a black band and the range of the unsaturated DENIS measurements as grey bands. Due to the variability the deviation from the blackbody in the variable region should not be taken as significant. *Bottom Right Panel:* An analog of the bottom left panel but for ‘post-burst’ photometric data. The sum of blackbodies has the same scale as the curve shown in the bottom left panel. The photometry is much more stable in the ‘post-outburst’ phase so we can somewhat safely interpret these points as representing the true SED.

using about 30 individual exposures for their total photometric measurement (Wright et al. 2010; Cutri & et al. 2012). V* CN Cha was observed as a strong point source in all four of the WISE photometric bands $W1$, $W2$, $W3$, and $W4$. More than 15% of the pixels were determined to be saturated in the $W1$ and $W2$ bands (Cutri & et al. 2012), thus we quote the measured photometry as lower bounds of the true flux at these wavelengths.

Once the cryogenic cooling on the WISE satellite became non-operational, observations could no longer be performed in the $W3$ and $W4$ bands, but the mission continued to observe the infrared sky in the $W1$ and $W2$ bands as the NEOWISE mission (Mainzer et al. 2014). While the NEOWISE mission observed V* CN Cha on several occasions, it was highly saturated in all exposures, having derived mean magnitudes of $W1 = 3.22$ and $W2 = 2.19$ mag, which is much brighter than the objects that NEOWISE was designed to measure (Mainzer et al. 2014). Regardless, we provide a further analysis of the lightcurve created by NEOWISE in Section 4.3.

2.15. SkyMapper

The SkyMapper Survey is a photometric survey of the southern sky performed on the 1.35-meter telescope at the Siding Spring Observatory in Australia. The survey uses six photometric bands, which are u , v , g , r , i , and z , and they had their first data release in January of 2018 (Wolf et al. 2018). V* CN Cha was not included in the stellar catalog of SkyMapper DR1 despite being observed in all six bands on three separate nights in March of 2014.

To make use of these data, we downloaded the images from the SkyMapper website⁵ and derived magnitudes based on reference to a nearby star which is reported in the stellar catalog of SkyMapper with magnitudes in all six bands. The reference star we used has associated SkyMapper ID 285891100 and *Gaia* ID 5199012694392465792. We then derived fluxes for V* CN Cha in the SkyMapper bands by using the AB zero-point magnitudes reported in Wolf et al. (2018). V* CN Cha was saturated in all SkyMapper exposures in the g , r , i , and z bands, so we only report measurements for the u and v bands. We derive $u = 9.08 \pm 0.20$ and $v = 8.59 \pm 0.17$ mag (in AB system) for V* CN Cha .

2.16. ASAS-SN

The All Sky Automated Survey for Supernovae (ASAS-SN) is a program aimed at searching for and monitoring bright supernovae in the variable sky

(Shappee et al. 2014). The project currently consists of 24 telescopes which monitor a large fraction of the night sky for variable sources down to magnitudes $V < 18$ ⁶. V* CN Cha was observed by ASAS-SN from December 28th, 2016 to February 9th, 2018 in the V band and was placed in the ASAS-SN variable star catalogue as a Gamma Cassiopeia (GCAS) variable star (Jayasinghe et al. 2019). Based on communication with the ASAS-SN team, this classification is probably not correct, in part due to the fact that V* CN Cha is quite bright for the range of magnitudes that ASAS-SN observes (Kochanek et al. 2017).

It is clear from the ASAS-SN light curve, shown on the right side of the top panel of Figure 2, that V* CN Cha remained at an almost constant magnitude of $V \sim 8$ mag for a significant portion of the ASAS-SN monitoring before beginning to dim by September of 2017. One may be worried that the constant magnitude region is simply due to saturation of the ASAS-SN observations. Again, based on communication with the ASAS-SN team, along with the fact that this measured magnitude is consistent with the G band magnitude measured by *Gaia*, this flat portion being due to saturation seems unlikely, but is still plausible (private communication, Tharindu Jayasinghe, ASAS-SN Team). We further analyze these data in Section 4.2.

2.17. Dark Energy Camera

V* CN Cha was observed by the Dark Energy Camera (DECam), an instrument created as part of the Dark Energy Survey (DES) (Abbott et al. 2018) and mounted on the Blanco 4-meter telescope at Cerro Tololo Inter-American Observatory (CTIO) in Chile. The observation was done as part of a search for substructure around the Magellanic clouds⁷. One exposure in the DES r -band, taken in June of 2016 is shown in Figure 1. V* CN Cha is clearly saturated on that image, so we did not derive photometric measurements.

2.18. TESS

The Transiting Exoplanet Survey Satellite (TESS) is a photometric survey satellite launched on April 18th of 2018 whose main scientific purpose is the discovery of exoplanets (Ricker et al. 2015). TESS observes single patches of the sky in 27.4 day segments, providing photometric measurements at a cadence of about 30 minutes. V* CN Cha was observed in TESS Sector 11 from April 22nd to May 20th of 2019.

⁵ <http://skymapper.anu.edu.au/image-cutout/>

⁶ <http://www.astronomy.ohio-state.edu/asasn/index.shtml>

⁷ <https://www.noao.edu/noaoprop/abstract.mpl?2016A-0366>

To determine the lightcurve (LC) of the star, we have extracted the 100x100 pixels cutouts from the calibrated full-frame images. The star has ~ 1200 observations. Since V* CN Cha has a nearby bright star $\sim 30''$ (1.4 pixels) away, we decided to do a simultaneous PSF fit of the 16×16 pixel area around the star throughout all the epochs, while including 3 nearby stars in the model, and allowing for small rotation and translation between individual images. The PSF model was a linear combination of two Gaussians oversampled at five times the pixel size of the image, that was allowed to vary from frame to frame. From this modeling we extract the lightcurve (LC) of V* CN Cha and of nearby stars. While the proper detrending and calibration of the LCs is beyond the scope of this paper, the extracted LCs of other stars in the field of V* CN Cha are quite constant with a typical median absolute deviation (MAD) of the LC of $< 0.5\%$, the MAD of the V* CN Cha LC is 2% and it shows an almost linear decline in flux by about 10% throughout the time of the TESS observations (27 days). That dimming corresponds to roughly a rate of 1.4 mag yr^{-1} (see Figure 3), which is consistent with the dimming starting at approximately Julian date 2458000 in the ASAS-SN lightcurve (see Figure 5).

3. DU PONT ECHELLE SPECTROSCOPY

The *Gaia* observations outlined above motivated our spectroscopic follow up with the Echelle Spectrograph on the 2.5-meter Irénée du Pont telescope at Las Campanas Observatory.⁸ This instrument provides coverage in the optical from $4000 - 9000 \text{ \AA}$ at $R \sim 40,000$. Our observations consisted of six exposures over 10 minutes from UTC 3:54 to UTC 4:08 on March 12th, 2019 (Julian date 2458554.672). We performed two 90 second exposures, three 60 second exposures and one 10 second exposure. The data was reduced using the Du Pont Echelle (DPE) reduction pipeline (publicly available online⁹). This reduction package makes use of the Carnegie Python Distribution (CarPy) which is also made available on the Carnegie Observatories Software Repository¹⁰ (Kelson et al. 2000; Kelson 2003).

The composite spectrum produced using all six exposures is shown in Figure 4. It is clear that the $H\alpha$ emission is quite broad and high equivalent width, making up the majority of the star's luminosity in the optical. While there are several other emission lines, the continuum flux is only detected at a signal-to-noise greater than 10 redward of approximately $\lambda \sim 4800 \text{ \AA}$. Among

the more obvious emission lines are the $H\beta$ and $H\gamma$ lines, which stand out clearly. We also tentatively identify several of the other prominent emission lines with Oxygen ([O I] 6300 & 6360 along with O I 8446 which is the second strongest line), Helium (He I 5875, 6678, and 7065), Nitrogen ([N II] 5756 & 6585), and Carbon (C I] 5317) and label these in Figure 4.

4. FURTHER DATA ANALYSIS

Here we present some calculations performed on the archival data and Du Pont spectrum that go beyond simply presenting the data as provided by the various survey teams. We title our subsections by the key physical take-aways.

4.1. *Mira Past*

It seems safe to conclude from several points of observation in the archival data laid out above that V* CN Cha was a Mira long-period variable star in its recent past. This is supported by its ASAS lightcurve shown at the left side of the top panel of Figure 2 and in detail in Figure 9. This observation is further supported by its archival identification as a Mira variable when it was first identified (Hoffmeister 1963), its identification as a likely variable by IRAS (Neugebauer et al. 1984), the NIR colors e.g. in 2MASS $J - K = 1.69 \text{ mag}$ (Epchtein et al. 1994; Skrutskie et al. 2006), and the RAVE spectrum gathered in early 2010 and discussed briefly in Section 2.10 (Kordopatis et al. 2013).

4.2. *Slowly Decaying Outburst*

Here we perform a more detailed analysis of the ASAS-SN lightcurve that was presented in Subsection 2.16. In particular we want to note the peak absolute magnitude and decay time, which are observables typically used to compare novae events to one another and are usually quantified using the extinction corrected, peak absolute magnitude in the V band ($M_{V,\text{peak}}^0 \text{ mag}$) and the time it takes for the event to decay by two magnitudes from this peak (t_2). Our analysis is illustrated in Figure 5.

We measure t_2 using a linear fit in magnitude space to the lightcurve for Julian Date greater than 2458000 days (the linear decay region). We then find the point at which this linear fit crosses two magnitudes decay from the peak observed apparent magnitude and define t_2 as the difference between that crossing time and the time that the peak magnitude was reached. We find $t_2 = 807 \text{ days}$.

We find $M_{V,\text{peak}}^0$ using the peak apparent magnitude observed in the ASAS-SN lightcurve ($m_{V,\text{peak}} = 7.773$). We then get the peak absolute magnitude using the *Gaia*

⁸ www.lco.cl/telescopes-information/irenee-du-pont

⁹ code.obs.carnegiescience.edu/dpe-pipeline

¹⁰ code.obs.carnegiescience.edu/carnegie-python-distribution

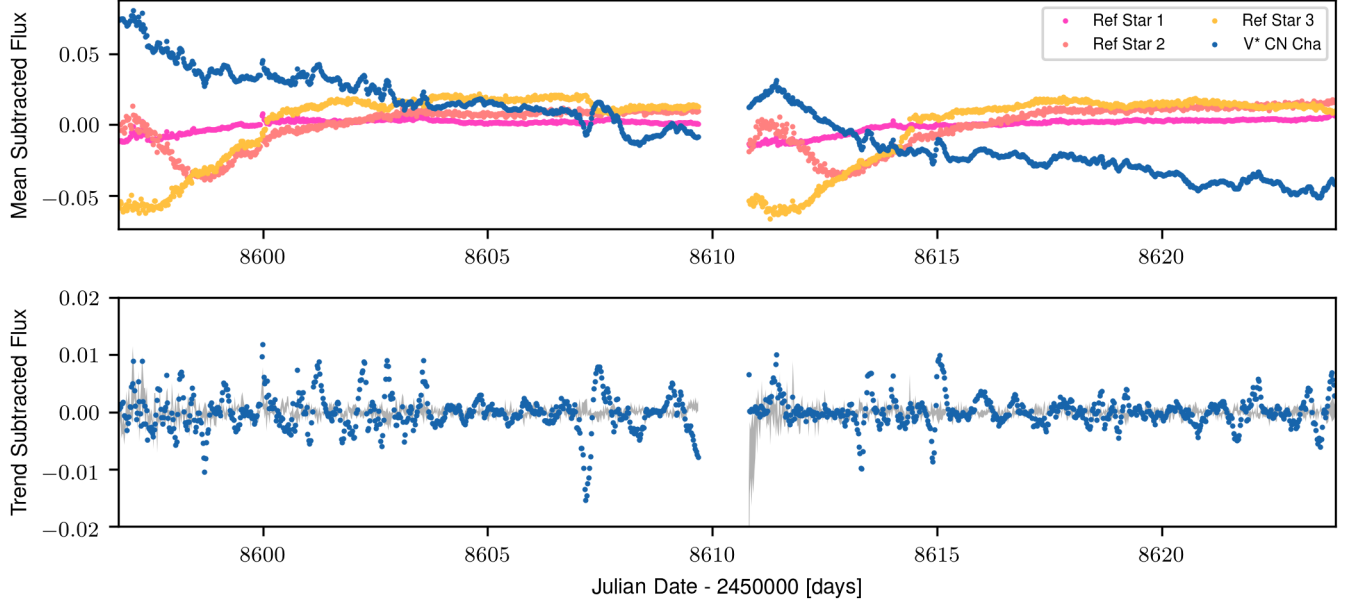


Figure 3. We show the lightcurve inferred from TESS photometry produced as described in Section 2.18. *Top Panel:* The mean-subtracted flux variations (in units of the logarithm of electron counts on the CCD detector) of V* CN Cha (blue) are compared against three comparison stars (pink and yellow). While all four sources show variations over time, the behavior of V* CN Cha is distinct from that of the reference stars, whose variations are likely due to TESS systematics. It is also clear that V* CN Cha is dimming over the course of the TESS observation, this dimming is still significant over periods where the reference stars are relatively constant in flux. *Bottom Panel:* We show the flux of V* CN Cha (blue) with a running mean on the scale of 10 hours subtracted out so as to make the short-period variations more visible. We additionally show the $1\text{-}\sigma$ variations in trend-corrected flux from the ‘ensemble’ of the three reference stars as the grey shaded region. It is clear that V* CN Cha has significant variation on the timescale of hours.

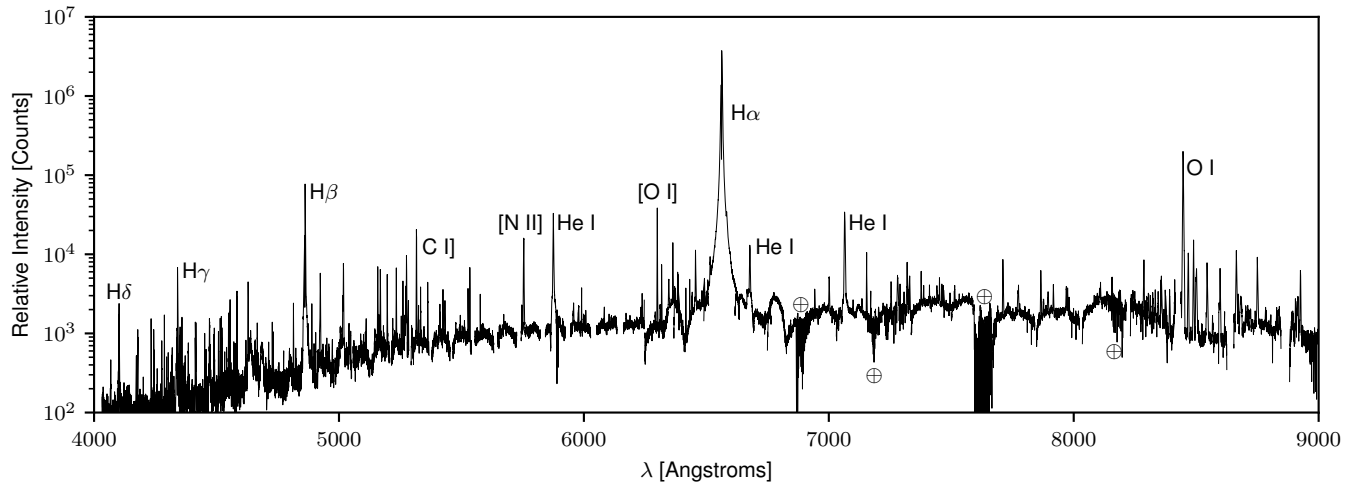


Figure 4. We show the optical spectrum of V* CN Cha observed using the Du Pont Echelle (DPE) instrument on the Irénée du Pont 2.5-meter telescope at Las Campanas Observatory on March 12th, 2019. This spectrum has been reduced using the CarPy software and the reduced spectrum has been divided by a normalized flat in order to account for the changing sensitivity as a function of wavelength. The vertical axis is then given at an arbitrary normalization which can roughly be interpreted as electron counts. We tentatively identify several of the emission lines, including several Helium, Nitrogen, and Oxygen lines and three of the Hydrogen Balmer lines. Regions of significant telluric absorption are indicated with the \oplus sign.

distance

$$M_{V,\text{peak}} = m_{V,\text{peak}} - 5 \log_{10} \left(\frac{d}{10 \text{ pc}} \right) = -4.74 \quad (3)$$

and correcting for extinction using $E(B - V) = 0.17$ mag from [Schlegel et al. \(1998\)](#) and $R_V = 3.1$ this gives us

$$M_{V,\text{peak}}^0 = M_{V,\text{peak}} - R_V E(B - V) = -5.27. \quad (4)$$

Finally, in order to get an estimate of the total amount of energy emitted during this outburst event, we calculate the total energy in the V band emitted over the course of the ASAS-SN observations. We do this by fitting a Gaussian Process (GP) regression, available through the `scikit learn` python package, to the extinction-corrected ($E(B - V) = 0.17$) ASAS-SN lightcurve ([Pedregosa et al. 2011](#)). This GP fit is shown (in observed magnitude space) in [Figure 5](#). We then integrate the fit GP over the full course of the ASAS-SN observation. Using this integral in combination with the *Gaia* distance and an effective wavelength for the V band of $\lambda_V = 5450 \text{ \AA}$ we derive the total energy in the V band of $E_V = 2.8 \times 10^{45}$ ergs.

4.3. Continued Bright Emission in MIR

Though the observations made by the NEOWISE mission of V^* CN Cha were saturated in all observations, we thought it useful to study the lightcurve if only to get a lower bound on the total amount of energy emitted in the $W1$ and $W2$ bands over the course of the NEOWISE observations. We restricted our analysis to photometric points from the NEOWISE catalog that were within $3.6''$ (0.001°) from V^* CN Cha and included the original WISE observations. The NEOWISE data are grouped, with several observations occurring over a few days semi-annually (roughly February and August 2014-2018). As these data are quite variable, we average all data points within each group to create a smoother overall lightcurve. We then integrate this lightcurve in a piecewise linear manner to get a total flux emitted over the observed period. We find 4.1×10^{45} ergs and 5.4×10^{45} ergs as lower bounds on the energy emitted in the $W1$ and $W2$ bands respectively. Additionally, there is no indication that the dimming that is seen in the V band is accompanied by dimming in the NEOWISE bands. If any effect is observed, it appears to become brighter in $W1$ and $W2$. This is hard to interpret given that the images are certainly in the non-linear regime.

4.4. Balmer Lines: Massive Outflow & Self-Absorption

It is clear from the spectrum that the star has an abnormally large Balmer decrement. In this subsection

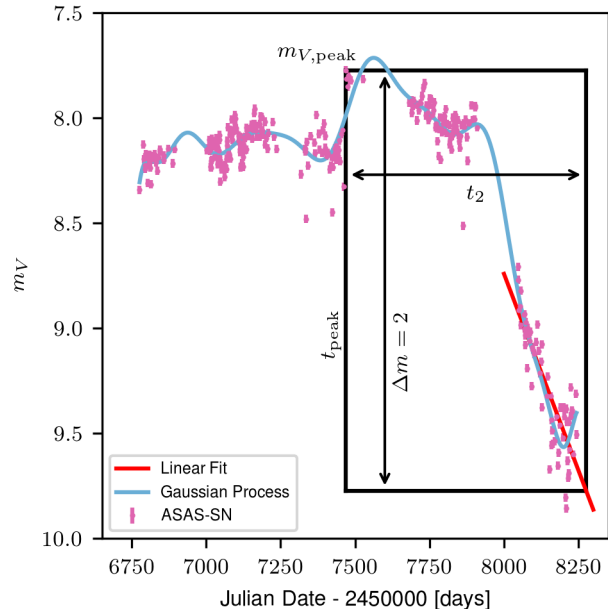


Figure 5. We present an in-depth look at the ASAS-SN lightcurve (shown in purple) for V^* CN Cha. We indicate the peak apparent magnitude (top of black box) time at which the peak magnitude is reached (left side of box), two magnitudes above the peak magnitude (bottom of box) and the time at which this occurs (right side of box). To find the time at which the lightcurve has decayed by two magnitudes we fit a linear decay to the ASAS-SN lightcurve points taken after Julian Day 2458000 and find where this fit (shown in red) crosses 2 mag above the peak apparent magnitude. We additionally we show a Gaussian Process fit to the data in light blue.

we will explore these lines in some detail, we first give quantitative measurements of the Balmer decrement and then use these numbers to infer the extinction needed to explain these decrements solely through dust absorption. We give phenomenological fits to the lines and the physical interpretation of these fits. Finally, we also calculate the equivalent widths of the lines.

Integrating the flux in each line and comparing we get $H\alpha/H\beta = 90.8$ (as opposed to the expected value of 3) and $H\gamma/H\beta \approx 0.08$ (typical value 0.45) ([Draine 2011](#)). We note that the $H\alpha$ emission was saturated in all exposures except for the 10 second exposure, so we use this exposure alone to measure the $H\alpha/H\beta$ ratio.

This abnormal Balmer decrement would usually be indicative of extensive reddening, however, as is noted in [Williams et al. \(2017\)](#), nebulae commonly exhibit strong Balmer decrements which can be due in large part to self-absorption in the higher order lines. We will come back to this in [Section 4.5](#). As a nebula is only one of the explanations we explore below, we will nonetheless

calculate the extinction that would be needed to explain the Balmer decrement that we see if there were no self-absorption. Estimating the extinction between the H α and H β lines as

$$E(\beta - \alpha) = 2.5 \log_{10} \left(\frac{1}{3} \frac{F_{\text{H}\alpha, \text{obs}}}{F_{\text{H}\beta, \text{obs}}} \right), \quad (5)$$

gives $E(\beta - \alpha) = 3.70$ mag. Similarly, we estimate $E(\gamma - \beta) = 1.86$ mag. Using the $R_V = 3.1$ extinction curve from Weingartner & Draine (2001), we can infer that this extinction would imply a visual extinction of $E(B - V)_{\text{Ba}} = 3.07$ mag, where we have used the subscript Ba to indicate that this extinction measurement comes from the Balmer decrement. Using this extinction measurement to correct the absolute *Gaia* G band magnitude calculated in section 2.2 would give an intrinsic magnitude of $G_0 = -14.4$ mag.

Even in the case that $E(B - V)_{\text{Ba}}$ is an accurate estimate of the true extinction, the above correction is not necessarily accurate given the abnormal distribution of light in the G band, as indicated by the Du Pont spectrum in Figure 4. However, this effect alone could not change the estimate given above enough to not make V* CN Cha intrinsically *very* bright if $E(B - V)_{\text{Ba}}$ were an accurate estimate of the extinction. For this reason it is reasonable to conclude that either $E(B - V)_{\text{Ba}}$ is not an accurate measure of the extinction *or* V* CN Cha is intrinsically as bright as a galaxy. While there have been transients with similar lifetimes and peak magnitudes as this, such as those found in the SPIRITS survey Kasliwal et al. (2017), we determine the former to be the more likely scenario.

In Figure 6 we show a zoom-in of the Balmer emission clearly visible in Figure 4. Note that while the lines are all displayed on the same scale, the H α line is reduced from the 10 sec exposure alone (since it is saturated in all other exposures) while the other lines are simply cutouts of Figure 4. It is clear from inspecting the Balmer lines that they all exhibit strong blue-shifted absorption in P-Cygni-like profiles. These profiles are typically indicative of a massive outflow of gas from the star. Each line is also very broad with widths on the order of 120 km s^{-1} (see below).

Attempts to fit the lines with either single Gaussian profiles or single Voigt profiles for the emission and absorption (over the wavelength regions shown in Figure 6) were unsuccessful. In an attempt to interpret these profiles shapes, we fit a five component Gaussian to each line. The model is defined as

$$F_{\text{mod}}(\nu) = F_{\text{emit}}(\nu) - F_{\text{abs}}(\nu), \quad (6)$$

where $F_{\text{mod}}(\nu)$ is the model prediction as a function of frequency, $F_{\text{emit}}(\nu)$ is the component dedicated to cap-

turing the emission profile and $F_{\text{abs}}(\nu)$ is the component meant to capture the absorption profile. We devote three Gaussians to the emission profile ($F_{\text{emit}}(\nu)$) and two Gaussians to the absorption profile ($F_{\text{abs}}(\nu)$). Within the emission or absorption profiles respectively all constituent Gaussians are enforced to have the same mean frequency, while all Gaussians are allowed to have different amplitudes and widths. The parameters of our model are then the central frequency of the emission profile (ν_e), the central frequency of the absorption profile (ν_a), the amplitudes of the Gaussians for the emission profile ($A_{e,1}, A_{e,2}, A_{e,3}$), the widths of the Gaussians for the emission profile ($\sigma_{e,1}, \sigma_{e,2}, \sigma_{e,3}$), the amplitudes of the Gaussians for the absorption profile ($A_{a,4}, A_{a,5}$), and the widths of the Gaussians for the absorption profile ($\sigma_{a,4}, \sigma_{a,5}$). This leaves us with 12 free parameters.

The physically relevant parameters of these fits are given in Table 1. The radial velocity shifts $\text{RV}_{\text{emit/abs}}$ are derived from the central frequencies of the fit profiles $\nu_{a/e}$ and the velocity Full-Width at Half-Maximum (FWHM) of the lines is derived by taking the frequency difference of the intersection of the profiles with their half-maximums. The dimensionless equivalent widths W , defined as

$$W = \int \frac{d\nu}{\nu_0} \left(1 - \frac{F_{\nu, \text{obs}}}{F_{\nu, 0}} \right), \quad (7)$$

where ν_0 is taken to be the rest frame wavelength of the particular line in air, $F_{\nu, \text{obs}}$ is the observed flux, and $F_{\nu, 0}$ is the background flux that would have been observed if the line were not present. We assume $F_{\nu, 0}$ to be a constant and go about estimating it by taking the two Echelle orders on either side of the line of interest, sigma-clipping them to remove smaller lines that may be present, and taking the mean of the resulting set of data. This method may not be entirely accurate for the H γ line, where the continuum is not detected at high signal-to-noise. Finally, the absorption-to-emission ratio given in Table 1 is estimated by integrating both the fitted emission and absorption profiles over the same wavelength regions used for the equivalent width estimates and taking the ratio of these integrals. We find the absorption to be between a half and a third of the emission across all lines.

4.5. $N \text{ II}$ Ratio Indicates High Density

We identify the emission lines [NII] 5756 and [NII] 6585, the latter of which sits on top of the wings of the H α line. The ratio of these emission lines can be used as a temperature diagnostic (Draine 2011). After subtracting out the background by fitting polynomials of degree 2 and 6 to the regions surrounding the [NII] 5756

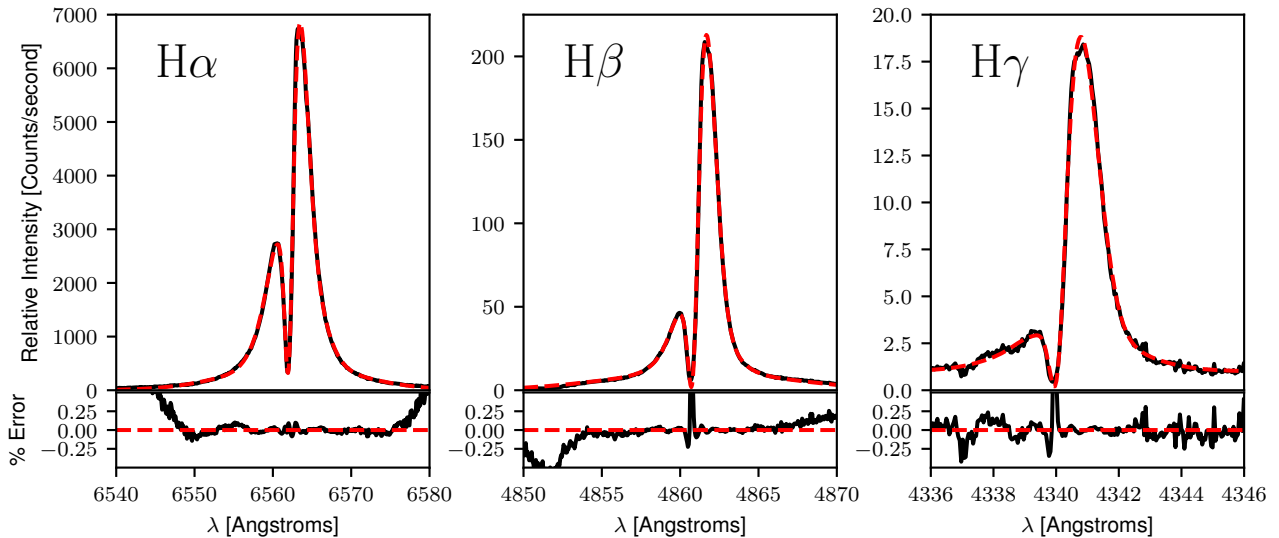


Figure 6. A zoom-in of the Balmer lines seen clearly in the spectrum shown in Figure 4. The data is shown in black while our five component Gaussian fit to the lines is shown as a red, dashed line. From left to right we show the $H\alpha$, $H\beta$, and $H\gamma$ lines. All lines are shown on the same scale, though the $H\alpha$ line is reduced purely from a 10 second exposure, as it was saturated in all 60 and 90 second exposures. The bottom panels show the residuals of the data relative to the five component Gaussian fit in terms of percent error. All lines are clearly quite broad and exhibit blue-shifted absorption, P-Cygni like, profiles.

Line	RV_{emit} [km/s]	RV_{abs} [km/s]	$(\Delta v)_{\text{FWHM,emit}}$ [km/s]	$(\Delta v)_{\text{FWHM,abs}}$ [km/s]	W	Absorption/Emission
$H\alpha$	-14.04 ± 0.46	-34.51 ± 0.19	166.74	89.03	-1.81	0.44
$H\beta$	-9.26 ± 1.12	-29.56 ± 0.18	121.34	72.65	-0.12	0.48
$H\gamma$	3.19 ± 2.67	-28.25 ± 0.28	118.35	59.26	-0.02	0.33

Table 1. The physically relevant parameters of our five-component Gaussian fit to the profiles of the Balmer lines shown in Figure 6. The first column specifies the line, columns 2 and 3 give the velocity blue-shifts which were fit to each of the lines in emission and absorption, while columns 4 and 5 give the Full-Width at Half-Maximum (FWHM) of the profiles for the lines in both emission and absorption. Column 6 gives the equivalent width of the line and column 7 gives the ratio of absorption to emission in the line, both calculated as explained in the text.

and $[\text{NII}] 6585$ lines respectively, we sum their fluxes and find a ratio of 2.385. If we additionally account for the extinction that occurs between these two lines based on the $E(B - V)$ from Schlegel et al. (1998) the line ratio becomes:

$$\frac{[\text{NII}]5756}{[\text{NII}]6585} = 2.583. \quad (8)$$

While, as just mentioned, this ratio is usually used as a temperature diagnostic, at such large values it is more useful as a density diagnostic (Draine 2011). Assuming a gas temperature of $T = 10^4$ K this ratio is indicative of an electron density of $n_e \gtrsim 10^7 \text{ cm}^{-3}$ (Draine 2011). These high densities would be consistent with self-absorption in the Hydrogen recombination lines that we posited in the last section (Netzer 1975; Drake & Ulrich 1980).

4.6. Dynamics of a Thick Disk Star

Here we review the dynamics of V^* CN Cha within the Galaxy that are derived from the astrometric measurement from Gaia Collaboration et al. (2018) and a radial velocity of ~ 0 km/s, motivated by our fits to the Balmer lines given in Subsection 4.4. This is laid out in Figure 8.

Though V^* CN Cha is spatially coincident on the sky with the Chamaeleon Complex, a star forming molecular cloud complex, lying between the Cha I ($\sim 2.5^\circ$ separation) and Cha III ($\sim 4^\circ$ separation) clouds, its distance as derived from its *Gaia* parallax ($3.18_{-0.23}^{+0.27}$ kpc) places it $20\times$ farther than the Chamaeleon Cloud (~ 180 pc) (Zucker et al. 2019). Furthermore, the proper motion of V^* CN Cha (a quantity that is in general much better measured by *Gaia*) is also inconsistent with the

proper motions of stars known to be associated with the Chamaeleon Complex. To be precise, the measured proper motion of V* CN Cha is $(\mu_{\alpha*}, \mu_{\delta}) = (-5.42, 7.02) \text{ mas yr}^{-1}$ while the proper motions of HD 97300 $((\mu_{\alpha*}, \mu_{\delta}) = (-21.01, -0.61) \text{ mas yr}^{-1})$ and HD 97048 $((\mu_{\alpha*}, \mu_{\delta}) = (-22.44, 1.31) \text{ mas yr}^{-1})$, both YSOs known to be associated with the Cha I cloud, are significantly different with the motion of V* CN Cha (Luhman 2008; Gaia Collaboration et al. 2018).

In Figure 8 we compare the past orbit of V* CN Cha with a star known to be in the Chamaeleon Cloud Complex (HD 97048) and the orbit of the Sun. It seems quite clear that V* CN Cha has dynamics that are consistent with a thick disk star, since the maximum vertical extent of its orbit is nearly 2 kpc above/below the disk plane and it is moving in a prograde fashion. More quantitatively, if we relate its vertical action $J_z = 75.3 \text{ kpc km s}^{-1}$ to its age using the thin disk vertical heating study of Ting & Rix (2019), the probability that this star is from the thin disk is negligible. This demonstrates that the star is most likely from the thick disk and therefore likely more than 8 Gyrs old.

4.7. Stochastic Optical Variability

We perform a power-spectrum analysis of the *TESS* light curve presented in Section 2.18 and displayed in Figure 3. We apply the *ASTROPY* Lomb-Scargle periodogram implementation (VanderPlas 2018) to the light curves from *TESS* Sectors 11 and 12 considered separately and together. Since strong *TESS* systematics occur on the timescale of its orbit (13.5 days), these are filtered out at the calibration stage of our analysis and therefore longer-timescale astrophysical variability is also removed.

The resulting power spectra are displayed in Figure 7 and the results are similar for the sectors treated independently. The spectrum decays with a red noise or ‘flicker’ profile above about 0.1 cycles per day; systematics on this timescale have been filtered out. The ‘flicker’ is consistent with stochastic variability, such as the turbulent motion of a convective photosphere or an accretion disk.

5. POSSIBLE EXPLANATIONS

Here we present possible explanations for the observations of this object that were outlined in Sections 2, 3, and 4. We present a simple comparison summary of how these theories explain the observations in Table 2. The theories explained below are ordered from least to most likely.

5.1. Young Stellar Object

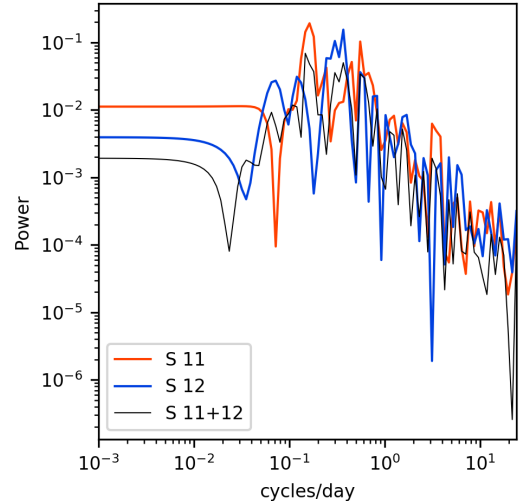


Figure 7. A power spectrum of the lightcurve taken by *TESS*, which is illustrated in Figure 7. The power spectrum of the data taken in Sector 11 of *TESS* is shown in red while that for Sector 12 is shown in blue. The joint power spectrum across both sectors is shown in black. All power spectra show red-noise which is indicative of stochastic variability.

Many characteristics of V* CN Cha seem to suggest we have caught a Young Stellar Object in outburst. In this case the main YSO candidates would be either a T Tauri star (Miller et al. 2011; Appenzeller & Mundt 1989), a Herbig Ae/Be star (Hillenbrand et al. 1992; Waters & Waelkens 1998), or an FU Orionis type star (Hartmann & Kenyon 1985, 1996). Indeed many new young stellar objects have been discovered using *Gaia* in combination with archival data (Hillenbrand et al. 2018, 2019a,b). In particular, the time-scale and relatively consistent brightness in the lightcurve post-outburst shown in the top panel of Figure 2 seem to be quite consistent with a period of increased accretion that is commonly seen in FU Ori type stars (Hartmann & Kenyon 1996).

There are two key observations which lead us to believe that a YSO is not a sufficient explanation of the data:

- (1) V* CN Cha appears to have been a Mira type long-period variable star from 1963 to as late as 2010, as laid out in Section 4.1. As far as we are aware, there is no YSO object that has photometric variability characteristic of a Mira.
- (2) The dynamics of the star, suggested by *Gaia* proper motions, indicate that the star is quite old. This is explained above in Section 4.6.

This evidence strongly indicates that V* CN Cha is not some kind of YSO. Though it is true that young

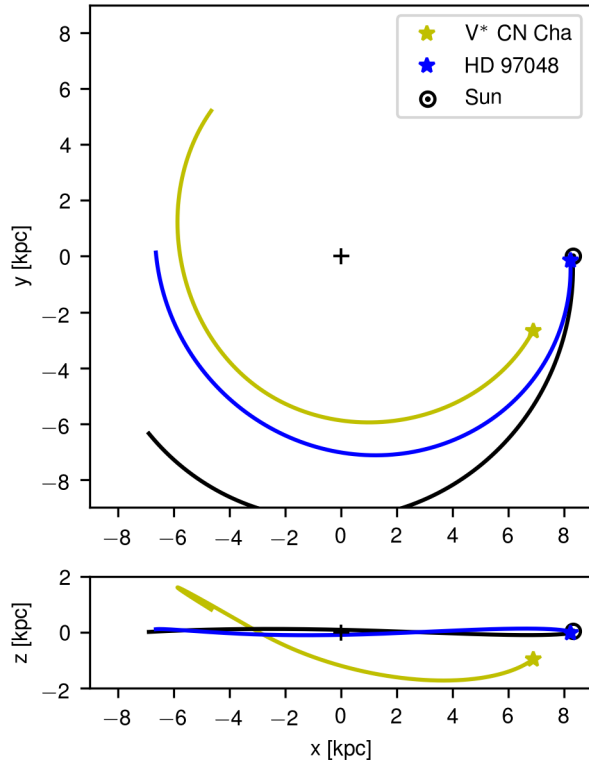


Figure 8. We show the galactic orbit of the star V* CN Cha (shown as a yellow star) along with the orbits of HD 97048 (a YSO known to be associated with the Chamaeleon Complex) in blue and the Sun in black. The top panel looks down up the disk plane, face-on while the bottom panel looks edge-on. The Galaxy is centered on the center of both panels. The orbits were integrated 100 Myrs back in time using `galpy` and the 2014 Milky Way Potential from [Bovy \(2015\)](#).

stars appear everywhere in our galaxy ([Price-Whelan et al. 2019](#)), they occur with much lower frequency outside of the disk plane ([Belokurov et al. 2019](#); [Binney & Tremaine 2008](#)). The fact that, based on *Gaia* dynamics, the last time that V* CN Cha crossed the mid-plane of the disk was 52.5 Myrs ago is a particularly bad sign for the YSO theory given our understanding of star formation mostly occurring in dense molecular clouds which are most common in the disk mid-plane ([McKee & Ostriker 2007](#)).

5.2. Protoplanetary Nebula

Another possible explanation for the phenomena we have outlined above would be the onset of the protoplanetary nebula (PPN) phase at the end of an evolved AGB cycle ([Kwok 1993](#)). While the observations of a massive outflow, combined with V* CN Cha being luminous in the infrared, and the presence of strong Hydrogen recombination lines, are consistent with a planetary nebula, the evolutionary timescales exhibited by V* CN

Cha are simply too short to be associated with a planetary nebula ([Marigo et al. 2001, 2004](#)). In particular, PPN theoretically should not show significant dimming from their peak magnitudes until several thousand years after the onset of the PPN phase ([Marigo et al. 2001](#)).

Additionally, our spectra of V* CN Cha exhibit no signs of the [O III]5007Å line that is ubiquitously present in all known planetary nebulae ([Méndez 2017](#)). This would tend to indicate that our system is much cooler than the typical proto-planetary nebula.

5.3. Symbiotic Nova

A symbiotic binary star is a binary star system consisting of an evolved star, usually a red giant branch (RGB) star or asymptotic giant branch (AGB) star, and a hot, compact companion, usually a white dwarf ([Mohamed & Podsiadlowski 2012](#); [Podsiadlowski & Mohamed 2007](#)). Binary systems with one component consisting of a white dwarf are thought to be the progenitors of classical novae, wherein hydrogen-rich material that is accreted from the binary companion on to the white dwarf triggers a thermonuclear runaway (TNR) ([Darnley & Henze 2019](#); [Starrfield et al. 2016](#)). Though most classical novae are thought to have late-type main sequence star companions ([Darnley & Henze 2019](#)), there are a few nova systems known to contain evolved star companions, and they particularly seem to make up the majority of known recurrent novae (RN), which have repeating outbursts on human-measurable timescales ([Patat et al. 2011](#); [Darnley et al. 2012](#)).

There are many characteristics that make the observations of V* CN Cha consistent with a nova occurring in a symbiotic binary system. The star clearly was classified as a Mira-type variable (an evolved AGB star [Catelan & Smith 2015](#)) for decades, explained in Section 4.1. The symbiotic binary theory would also explain the UV excess exhibited by the UVOT observations, visible in the bottom-left panel of Figure 2, and fit by a 10000 K blackbody. The stochastic variability observed in the *TESS* lightcurve and analyzed in detail in Section 4.7 is well explained by an accretion disk around the white dwarf companion. This explanation would additionally be consistent with the dynamics of the star outlined in Figure 8, which indicate it is an old thick-disk star.

While the timescale of decline for the lightcurve of V* CN Cha as presented by the ASAS-SN data is somewhat abnormal for novae in general (typically on the order of tens of days), it is not abnormal for symbiotic novae. In particular, V* CN Cha has a timescale that is quite similar to the Symbiotic Nova in PU Vul, which declined over thousands of days [Mikolajewska \(2010\)](#). The timescale for decline is also quite similar to sev-

eral mid-infrared transients which have been observed in extragalactic surveys (Kasliwal et al. 2017).

6. DISCUSSION

Of the explanations presented in Section 5 we believe that a symbiotic novae is most consisted with the wide range of observations we have gathered on V* CN Cha. In this section, we briefly discuss the implications for the interpretation of V* CN Cha as a symbiotic nova.

One of the key empirical insights that has resulted from the study of classical novae is the relationship between their peak magnitudes and the time-scale over which they decay, known as the Maximum Magnitude Rate of Decline (MMRD) relation (Downes & Duerbeck 2000). This empirical relationship shows that brighter novae decay more quickly to their pre-nova magnitudes. The mass of the white dwarf in the system is thought to drive the MMRD (e.g., Livio 1992), such that the higher the white dwarf mass is, the higher the surface gravity and hence the higher the pressure in the white dwarf atmosphere, causing a stronger thermonuclear runaway (TNR) and therefore a brighter peak luminosity. At the same time, at higher white dwarf mass the less massive the atmosphere needs to be before TNR is triggered, causing the nova to decay more quickly, as it has less fuel.

The discovery in recent years of several novae that fall off of the MMRD relation has called into question the simple argument outlined above (Kasliwal et al. 2011; Shara et al. 2017). This has mainly been driven by the further study of galactic recurrent novae (Hachisu & Kato 2019) and the discovery of so-called ‘faint-fast’ novae in M31 and M87. In particular, it has been argued that the MMRD should at the very least depend upon some details of the donor star as well as the white dwarf’s temperature and composition.

If we take the peak absolute magnitude in the V band of V* CN Cha to be $M_{V,\text{peak}}^0 = -5.27$ mag and its time-scale to decay from this peak by two magnitudes to be $t_2 = 807$ days (calculations outlined in Section 4.2), the outburst we observe would be one of the longest decays currently measured for novae. The most direct comparison, is the Galactic symbiotic nova, PU Vul, and some infrared-discovered extragalactic transients (Mikolajewska 2010; Kasliwal et al. 2017). Furthermore, V* CN Cha is among the lowest luminosity of any known nova, roughly tying for this distinction with novae 39-41 of Shara et al. (2016).

Symbiotic binary systems are also thought to be possible progenitors for Type Ia supernovae (Patat et al. 2011; Hachisu et al. 1999). Recent work has even suggested that mass accretion onto the compact compan-

ion via so-called Wind Roche-Lobe Overflow (WRLOF) could make these binary systems even more likely to create supernovae (Mohamed & Podsiadlowski 2007; Ilkiewicz et al. 2019). In this context, V* CN Cha may be able to provide interesting insights in to the viability of this progenitor channel for Type Ia supernovae.

7. SUMMARY AND FOLLOW-UP

We have presented and organized the various archival data on the stellar object V* CN Cha in the constellation of Chamaeleon. We used these observations to motivate that the luminosity from V* CN Cha was dominated by a Mira long-period variable star from 1963 until 2013, at which point the star seemed to enter an outburst phase. After remaining at roughly a constant luminosity for about 3 years, the object then entered a dimming phase, during which time it dimmed at about 1.4 magnitudes per year.

We then presented the optical spectrum that motivated our initial interest in this system. The spectrum is dominated by emission in hydrogen recombination lines, predominantly from $H\alpha$. The Balmer series lines exhibit blue-shifted absorption, indicative of a massive outflow from the object. The spectrum additionally presents emission lines of He I, C I], [N II], O I, and [O I], among many others that we did not explicitly identify. Many of these lines exhibit complicated profiles.

We estimate the electron density of the environment using the ratio of [N II] forbidden lines and we find a density of $n_e \gtrsim 10^7 \text{ cm}^{-3}$. We additionally concluded that the extreme Balmer decrement seen in our spectrum was most likely not due to extinction but due to self-absorption; this is consistent with the high densities indicated by the [N II] ratio. We made phenomenological fits to the profiles of the Balmer series lines which indicated large velocity widths (~ 120 km/s) and outflow velocities from the absorption of ~ 20 km/s. We additionally provide an analysis of the peak magnitude and decay time of the outburst, indicating a rather long period and low peak-luminosity compared to other novae outbursts. Finally, we showed that the dynamics of the object, as inferred from the *Gaia* astrometry and a radial velocity, indicate an old star, perhaps a component of the thick disk (lying 1 kpc below the disk mid-plane).

After considering that V* CN Cha may be either a young stellar object or an early phase protoplanetary nebula, we used the evidence summarized above to argue that the data are best explained by a nova occurring in a symbiotic binary system. If this is indeed the case, the V* CN Cha outburst would be among the lowest luminosity novae ever documented (tied with novae 39-41

Theory	Mira Variability	UV Excess	Outburst Timescale	Balmer Decrement	Dynamics/ Age	Balmer Line Strength
YSO	X	✓	✓	X	X	?
pPN	✓	?	X	?	✓	?
Symbiotic Nova	✓	✓	✓	?	✓	?

Table 2. We give a simple comparison between the key observations we have described and the theories we have proposed for explaining them. A ✓ indicates that the theory explains the observation, a X indicates that the theory does not explain the observation, and a ? indicates that it is uncertain whether or not the theory explains the observation.

of Shara et al. (2016)), providing interesting new context to the MMRD relation for novae.

More concrete conclusions will be drawn about this object from an in-depth analysis of the spectral data that we have gathered, including follow-up high-cadence spectra at both high and moderate resolution that we gathered in late November/early December of 2019. We reserve detailed analyses of this data to future work.

We will be also able to learn a great deal more about this object’s evolution over the course of its outburst once the *Gaia* BP/RP spectra (which cover almost the entirety of the outburst phase) are released to the community; this is anticipated with *Gaia* DR3 planned for late 2021. Supplementing our current data with observations in the radio and X-ray will be extremely informative in discerning between the different scenarios we have proposed here.

As we pointed out in the introduction to this manuscript, there is no single database that encapsulates the vast array of human-collected astronomical data. We believe that the discovery we have described in this work presents a concrete example of the consequences of not having such a resource. Though nearly all of the information that made this object interesting was freely available to the community, it was scattered between many catalogs, interfaces, and repositories. As a result, this object was overlooked and its discovery was serendipitous. This paper by no means constitutes the sole such example (Hillenbrand et al. 2018, 2019a,b).

This problem will only become worse in the near future with large upcoming time-domain astronomical surveys such as the Vera C. Rubin Observatory (VRO, formerly LSST) and large spectroscopic surveys such as SDSS-V, *WEAVE*, and *4MOST* (Ivezić et al. 2019; Kollmeier et al. 2017; Bonifacio et al. 2016; de Jong et al. 2019). We believe that the importance of well thought-out and easily searchable/accessible data will be paramount in the coming astronomical age, and that doing this correctly should be considered a priority for the community.

The desire for a tool that would facilitate the access of data across surveys of widely varying structure is certainly not a new concept. In fact, this study has

made use of several such tools intended for this purpose and developed over the past generation, including: the “Whole Sky Database” created by Sergey Koposov and maintained at the University of Cambridge (Koposov & Bartunov 2006), the SIMBAD database created by the Centre de Données astronomique de Strasbourg (CDS) (Wenger et al. 2000), the Vizier online database of catalogues (Ochsenbein et al. 2000), and the sky visualizer Aladin Bonnarel et al. (2000). There have been several other great efforts made by researchers along these lines including the National Virtual Observatory (Szalay 2001), the CDS overall (Egret & Albrecht 1995; Genova et al. 1996), the Mikulski Archive for Space Telescopes (MAST) (Rafelski et al. 2019) along with too many others to give a complete list here.

Despite the largely successful efforts of these programs, we believe this work demonstrates that there are still regions of discovery which are made less accessible by the lack of a perfectly effective cross-survey search tool. Though it is difficult to find and characterize anomalous objects, these objects have the potential to make us fundamentally reconsider our understanding of the world around us. We look forward to an age of astronomy in which these discoveries can be made commonplace.

The authors would like to thank Howard Bond, Matteo Cantiello, and Adam Jermyn for pointing us towards symbiotic binary systems as a possible explanation for this object and for further useful discussions on the nature of the object. We would additionally like to thank Michael Shara for recommending relevant literature references with regards to symbiotic novae as novae in general. We would like to thank Tharindu Jayasinghe and Krzysztof Stanek for consulting us on the ASAS-SN observations. We would like to thank Arne Henden and Sara Beck for consulting us on the APASS measurements. The authors would additionally like to thank Gaspar Bakos, Adam Burrows, Trevor David, Bruce Draine, Andy Goulding, Emily Levesque, Erin Kado-Fong, Eliot Quataert, Nathan Smith, David Spergel, Joshua Winn, and Vasily Belokurov, Wyn Evans and the other members of the Cambridge Streams group for

useful conversations and references. L.L. would like to thank the Center for Computational Astrophysics at the Flatiron Institute in New York City for their hospitality while part of this work was completed.

This work was performed in part under contract with the Jet Propulsion Laboratory (JPL) funded by NASA through the Sagan Fellowship Program executed by the NASA Exoplanet Science Institute. Support for this work was provided by NASA through Hubble Fellowship grant #51386.01 awarded to R.L.B. and grant #51425.001 awarded to Y.S.T. by the Space Telescope Science Institute, which is operated by the Association of Universities for Research in Astronomy, Inc., for NASA, under contract NAS 5-26555. SK is partially supported by NSF grants AST-1813881, AST-1909584 and Heising-Simons foundation grant 2018-1030.

This publication makes use of data products from the Wide-field Infrared Survey Explorer, which is a joint project of the University of California, Los Angeles, and the Jet Propulsion Laboratory/California Institute of Technology, funded by the National Aeronautics and Space Administration.

This work has made use of data from the European Space Agency (ESA) mission *Gaia* ([https://www.](https://www.cosmos.esa.int/gaia)

[cosmos.esa.int/gaia](https://www.cosmos.esa.int/gaia)), processed by the *Gaia* Data Processing and Analysis Consortium (DPAC, <https://www.cosmos.esa.int/web/gaia/dpac/consortium>). Funding for the DPAC has been provided by national institutions, in particular the institutions participating in the *Gaia* Multilateral Agreement.

This research made use of NASA’s Astrophysics Data System and the SIMBAD database, operated at CDS, Strasbourg, France. Some of the data presented in this paper were obtained from the Mikulski Archive for Space Telescopes (MAST). STScI is operated by the Association of Universities for Research in Astronomy, Inc., under NASA contract NAS5-26555. Support for MAST for non-HST data is provided by the NASA Office of Space Science via grant NNX13AC07G and by other grants and contracts.

This paper made use of the Whole Sky Database (wsdb) created by Sergey Koposov and maintained at the Institute of Astronomy, Cambridge by Sergey Koposov, Vasily Belokurov and Wyn Evans with financial support from the Science & Technology Facilities Council (STFC) and the European Research Council (ERC).

APPENDIX

A. ASAS CATALOGUES

Here we briefly discuss the two separate photometric catalogues that we found describing the light curve of V* CN Cha based on the ASAS survey. The first, which included photometric data up October 11th, 2003, was obtained from the online catalogue *Vizier* (catalogue 1) (Pojmanski 2002b). The second catalogue is the “ASAS All Star Catalogue” (catalogue 2) which is hosted on servers at the University of Washington (Pojmanski 2010). This second catalogue contains photometric information over the full range of observations, with magnitudes obtained through measurement in four separate apertures. When using the data we simply take the error-weighted mean of these four measurements.

When looking at the data in catalogue 2 which was taken during the same time interval as is covered in catalogue 1, one would expect these data to agree with one another. However, there seem to be several data points in catalogue 2 which do not appear in catalogue 1 and vice versa. Additionally, there are some minor inconsistencies in magnitudes between measurements in each catalogue that are meant to be measured at the same time. As we weren’t able to resolve which of these measurements to trust more, we use the data given in both catalogues here. A comparison of the two catalogues, over the period covered by catalogue 1, is given in Figure 9.

REFERENCES

- 1997, The HIPPARCOS and TYCHO catalogues. Astrometric and photometric star catalogues derived from the ESA HIPPARCOS Space Astrometry Mission, Vol. 1200
- Abbott, T. M. C., Abdalla, F. B., Alarcon, A., et al. 2018, *PhRvD*, 98, 043526
- Appenzeller, I., & Mundt, R. 1989, *A&A Rv*, 1, 291
- Belokurov, V., Sanders, J. L., Fattahi, A., et al. 2019, arXiv e-prints, arXiv:1909.04679
- Binney, J., & Tremaine, S. 2008, *Galactic Dynamics: Second Edition*
- Bonifacio, P., Dalton, G., Trager, S., et al. 2016, in *SF2A-2016: Proceedings of the Annual meeting of the French Society of Astronomy and Astrophysics*, ed. C. Reylé, J. Richard, L. Cambrésy, M. Deleuil, E. Pécontal, L. Tresse, & I. Vauglin, 267–270
- Bonnarel, F., Fernique, P., Bienaymé, O., et al. 2000, *A&AS*, 143, 33

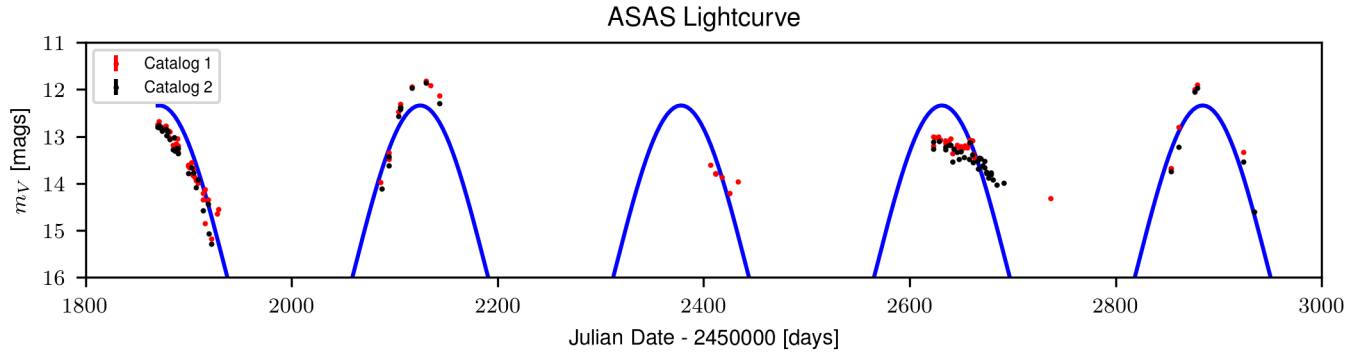


Figure 9. We show the ASAS light curve for V* CN Cha in the V band for both catalogue 1 (red points) and catalogue 2 (black points) as referred to in the text, though only over the period covered by catalogue 1. Both catalogues have typical photometric errors of 0.02 magnitudes. To guide the eye we also include a sine curve with a period of 253.24 days and a mean of 12.34 mags (as determined by the original ASAS team, blue curve) we fit for the optimal phase shift and amplitude (3.43 mags).

- Bovy, J. 2015, *ApJS*, 216, 29
- Catelan, M., & Smith, H. A. 2015, *Pulsating Stars*
- Cutri, R. M., & et al. 2012, *VizieR Online Data Catalog*, II/311
- Darnley, M. J., & Henze, M. 2019, arXiv e-prints, arXiv:1909.10497
- Darnley, M. J., Ribeiro, V. A. R. M., Bode, M. F., Hounsell, R. A., & Williams, R. P. 2012, *ApJ*, 746, 61
- de Jong, R. S., Agertz, O., Berbel, A. A., et al. 2019, *The Messenger*, 175, 3
- DENIS Consortium. 2005, *VizieR Online Data Catalog*, II/263
- Downes, R. A., & Duerbeck, H. W. 2000, *AJ*, 120, 2007
- Draine, B. T. 2011, *Physics of the Interstellar and Intergalactic Medium* (Princeton University Press). <http://www.jstor.org/stable/j.ctvcvm4hzr>
- Drake, S. A., & Ulrich, R. K. 1980, *ApJS*, 42, 351
- Egret, D., & Albrecht, M. A. 1995, *Information & on-line data in astronomy*, doi:10.1007/978-94-011-0397-8
- Epchtein, N., de Batz, B., Copet, E., et al. 1994, *Ap&SS*, 217, 3
- Fouqué, P., Chevallier, L., Cohen, M., et al. 2000, *A&AS*, 141, 313
- Gaia Collaboration, Prusti, T., de Bruijne, J. H. J., et al. 2016, *A&A*, 595, A1
- Gaia Collaboration, Brown, A. G. A., Vallenari, A., et al. 2018, *A&A*, 616, A1
- Genova, F., Bartlett, J. G., Bienaymé, O., et al. 1996, *Vistas in Astronomy*, 40, 429
- Hachisu, I., & Kato, M. 2019, *ApJS*, 242, 18
- Hachisu, I., Kato, M., & Nomoto, K. 1999, *ApJ*, 522, 487
- Hartmann, L., & Kenyon, S. J. 1985, *ApJ*, 299, 462
- . 1996, *ARA&A*, 34, 207
- Henden, A., & Munari, U. 2014, *Contributions of the Astronomical Observatory Skalnaté Pleso*, 43, 518
- Henden, A. A., Levine, S., Terrell, D., et al. 2018, in *American Astronomical Society Meeting Abstracts*, Vol. 232, American Astronomical Society Meeting Abstracts #232, 223.06
- Henden, A. A., Welch, D. L., Terrell, D., & Levine, S. E. 2009, in *American Astronomical Society Meeting Abstracts*, Vol. 214, American Astronomical Society Meeting Abstracts #214, 407.02
- Hillenbrand, L. A., Reipurth, B., Connelley, M., Cutri, R. M., & Isaacson, H. 2019a, arXiv e-prints, arXiv:1910.05790
- Hillenbrand, L. A., Strom, S. E., Vrba, F. J., & Keene, J. 1992, *ApJ*, 397, 613
- Hillenbrand, L. A., Contreras Peña, C., Morrell, S., et al. 2018, *ApJ*, 869, 146
- Hillenbrand, L. A., Miller, A. A., Carpenter, J. M., et al. 2019b, *ApJ*, 874, 82
- Hoffmeister, C. 1963, *Veröffentlichungen der Sternwarte Sonneberg*, 6, 1
- Høg, E., Fabricius, C., Makarov, V. V., et al. 2000, *A&A*, 355, L27
- Ikiewicz, K., Mikołajewska, J., Belczyński, K., Wiktorowicz, G., & Karczmarek, P. 2019, *MNRAS*, 485, 5468
- Ivezić, Ž., Kahn, S. M., Tyson, J. A., et al. 2019, *ApJ*, 873, 111
- Jayasinghe, T., Stanek, K. Z., Kochanek, C. S., et al. 2019, arXiv e-prints, arXiv:1907.10609
- Jester, S., Schneider, D. P., Richards, G. T., et al. 2005, *AJ*, 130, 873
- Kasliwal, M. M., Cenko, S. B., Kulkarni, S. R., et al. 2011, *ApJ*, 735, 94
- Kasliwal, M. M., Bally, J., Masci, F., et al. 2017, *ApJ*, 839, 88
- Kelson, D. D. 2003, *PASP*, 115, 688

- Kelson, D. D., Illingworth, G. D., van Dokkum, P. G., & Franx, M. 2000, *ApJ*, 531, 159
- Kochanek, C. S., Shappee, B. J., Stanek, K. Z., et al. 2017, *PASP*, 129, 104502
- Kollmeier, J. A., Zasowski, G., Rix, H.-W., et al. 2017, arXiv e-prints, arXiv:1711.03234
- Koposov, S., & Bartunov, O. 2006, *Astronomical Society of the Pacific Conference Series*, Vol. 351, Q3C, Quad Tree Cube – The new Sky-indexing Concept for Huge Astronomical Catalogues and its Realization for Main Astronomical Queries (Cone Search and Xmatch) in Open Source Database PostgreSQL, ed. C. Gabriel, C. Arviset, D. Ponz, & S. Enrique, 735
- Kordopatis, G., Gilmore, G., Steinmetz, M., et al. 2013, *AJ*, 146, 134
- Kuin, N. P. M., Landsman, W., Breeveld, A. A., et al. 2015, *MNRAS*, 449, 2514
- Kwok, S. 1993, *ARA&A*, 31, 63
- Lasker, B. M., Doggett, J., McLean, B., et al. 1996, in *Astronomical Society of the Pacific Conference Series*, Vol. 101, *Astronomical Data Analysis Software and Systems V*, ed. G. H. Jacoby & J. Barnes, 88
- Lasker, B. M., Sturch, C. R., McLean, B. J., et al. 1990, *AJ*, 99, 2019
- Livio, M. 1992, *Astronomical Society of the Pacific Conference Series*, Vol. 29, *White Dwarf Masses in Nova Systems and the Maximum-Magnitude vs. Rate-of-Derivative Relation*, ed. N. Vogt, 4
- Luhman, K. L. 2008, *Chamaeleon*, ed. B. Reipurth, Vol. 5, 169
- Mainzer, A., Bauer, J., Cutri, R. M., et al. 2014, *ApJ*, 792, 30
- Marigo, P., Girardi, L., Groenewegen, M. A. T., & Weiss, A. 2001, *A&A*, 378, 958
- Marigo, P., Girardi, L., Weiss, A., Groenewegen, M. A. T., & Chiosi, C. 2004, *A&A*, 423, 995
- McKee, C. F., & Ostriker, E. C. 2007, *ARA&A*, 45, 565
- Méndez, R. H. 2017, in *IAU Symposium*, Vol. 323, *Planetary Nebulae: Multi-Wavelength Probes of Stellar and Galactic Evolution*, ed. X. Liu, L. Stanghellini, & A. Karakas, 298–302
- Mikolajewska, J. 2010, arXiv e-prints, arXiv:1011.5657
- Miller, A. A., Hillenbrand, L. A., Covey, K. R., et al. 2011, *ApJ*, 730, 80
- Milne, A. A. 1956, *The Complete Tales of Winnie-the-Pooh* (Dutton Children's Books)
- Mohamed, S., & Podsiadlowski, P. 2007, *Astronomical Society of the Pacific Conference Series*, Vol. 372, *Wind Roche-Lobe Overflow: a New Mass-Transfer Mode for Wide Binaries*, ed. R. Napiwotzki & M. R. Burleigh, 397
- . 2012, *Baltic Astronomy*, 21, 88
- Murakami, H., Baba, H., Barthel, P., et al. 2007, *PASJ*, 59, S369
- Netzer, H. 1975, *MNRAS*, 171, 395
- Neugebauer, G., Habing, H. J., van Duinen, R., et al. 1984, *ApJL*, 278, L1
- Ochsenbein, F., Bauer, P., & Marcout, J. 2000, *A&AS*, 143, 23
- Page, M. J., Yershov, V., Breeveld, A., et al. 2014, in *Proceedings of Swift: 10 Years of Discovery (SWIFT 10)*, held 2-5 December 2014 at La Sapienza University, Rome, Italy. Online at <http://pos.sissa.it/cgi-bin/reader/conf.cgi?confid=233> <http://pos.sissa.it/cgi-bin/reader/conf.cgi?confid=233i/Ai>, id.37, 37
- Patat, F., Chugai, N. N., Podsiadlowski, P., et al. 2011, *A&A*, 530, A63
- Pedregosa, F., Varoquaux, G., Gramfort, A., et al. 2011, *Journal of Machine Learning Research*, 12, 2825
- Podsiadlowski, P., & Mohamed, S. 2007, *Baltic Astronomy*, 16, 26
- Pojmanski, G. 1997, *AcA*, 47, 467
- . 2002a, *AcA*, 52, 397
- . 2002b, *ASAS Variable Stars in Southern hemisphere*, *VizieR*. <http://vizier.u-strasbg.fr/viz-bin/VizieR-3?-source=II/264/var>
- . 2003, *AcA*, 53, 341
- . 2004, arXiv e-prints, astro
- . 2010, *ASAS All Star Catalogue*, University of Washington. <http://www.astrouw.edu.pl/asas/?page=aasc>
- Price-Whelan, A. M., Nidever, D. L., Choi, Y., et al. 2019, *ApJ*, 887, 19
- Rafelski, M., Cherinka, B., Smith, A. M., Peek, J., & Hargis, J. 2019, in *American Astronomical Society Meeting Abstracts*, Vol. 233, *American Astronomical Society Meeting Abstracts #233*, 157.30
- Ricker, G. R., Winn, J. N., Vanderspek, R., et al. 2015, *Journal of Astronomical Telescopes, Instruments, and Systems*, 1, 014003
- Schlegel, D. J., Finkbeiner, D. P., & Davis, M. 1998, *ApJ*, 500, 525
- Shappee, B. J., Prieto, J. L., Grupe, D., et al. 2014, *ApJ*, 788, 48
- Shara, M. M., Doyle, T. F., Lauer, T. R., et al. 2016, *ApJS*, 227, 1
- Shara, M. M., Doyle, T., Lauer, T. R., et al. 2017, *ApJ*, 839, 109
- Skrutskie, M. F., Cutri, R. M., Stiening, R., et al. 2006, *AJ*, 131, 1163

- Starrfield, S., Iliadis, C., & Hix, W. R. 2016, *PASP*, 128, 051001
- Szalay, A. S. 2001, *Astronomical Society of the Pacific Conference Series*, Vol. 238, *The National Virtual Observatory*, ed. J. Harnden, F. R., F. A. Primini, & H. E. Payne, 3
- Ting, Y.-S., & Rix, H.-W. 2019, *ApJ*, 878, 21
- VanderPlas, J. T. 2018, *ApJS*, 236, 16
- Vogt, N., Contreras-Quijada, A., Fuentes-Morales, I., et al. 2016, *ApJS*, 227, 6
- Waters, L. B. F. M., & Waelkens, C. 1998, *ARA&A*, 36, 233
- Weingartner, J. C., & Draine, B. T. 2001, *ApJ*, 548, 296
- Wenger, M., Ochsenbein, F., Egret, D., et al. 2000, *A&AS*, 143, 9
- Williams, S. C., Darnley, M. J., & Henze, M. 2017, *MNRAS*, 472, 1300
- Wolf, C., Onken, C. A., Luvaul, L. C., et al. 2018, *PASA*, 35, e010
- Wright, E. L., Eisenhardt, P. R. M., Mainzer, A. K., et al. 2010, *AJ*, 140, 1868
- Yamamura, I., Makiuti, S., Ikeda, N., et al. 2010, *VizieR Online Data Catalog*, II/298
- Yershov, V. N. 2014, *Ap&SS*, 354, 97
- Zucker, C., Speagle, J. S., Schlafly, E. F., et al. 2019, *ApJ*, 879, 125